

Observational Study



Local Brain Activity Differences Between Herpes Zoster and Postherpetic Neuralgia Patients: A Resting-State Functional MRI Study

Song Cao, MD, PhD^{1,3}, Ying Li, MD¹, Wenwen Deng, MD^{4,5}, Bangyong Qin, MD¹, Yi Zhang, MD, PhD^{1,2}, Peng Xie, MD, PhD², Jie Yuan, MD, PhD², Buwei Yu, MD, PhD³, and Tian Yu, MD^{1,2}

From: ¹Department of Anesthesiology, Zunyi Medical College, Zunyi, Guizhou, China; ²Guizhou Key Laboratory of Anesthesia and Organ Protection, Zunyi, Guizhou, China; ³Department of Anesthesiology, Ruijin Hospital of Shanghai Jiaotong University School of Medicine, Shanghai, China; ⁴Department of Cardiology, Affiliated Hospital of Zunyi Medical College, Zunyi, Guizhou, China; ⁵Department of Radiology, Affiliated Hospital of Zunyi Medical College, Zunyi, Guizhou, China

Address Correspondence:
Tian Yu, MD, PhD

Department of Anesthesiology
Zunyi Medical College
201 Dalian Road, Zunyi, 563000,
Guizhou, China
E-mail: zyyutian@126.com
Buwei Yu, MD, PhD

Department of Anesthesiology
Ruijin Hospital of Shanghai Jiaotong
University School of Medicine
Shanghai, China
E-mail: ruijin_yubw@163.com

Disclaimer: There was no external funding in the preparation of this manuscript.

Conflict of interest: Each author certifies that he or she, or a member of his or her immediate family, has no commercial association (i.e., consultancies, stock ownership, equity interest, patent/licensing arrangements, etc.) that might pose a conflict of interest in connection with the submitted manuscript.

Manuscript received: 10-14-2016
Revised manuscript received:
01-01-2017
Accepted for publication:
01-12-2017

Free full manuscript:
www.painphysicianjournal.com

Background: Herpes zoster (HZ) can develop into postherpetic neuralgia (PHN), both of which are painful diseases. PHN patients suffer chronic pain and emotional disorders. Previous studies showed that the PHN brain displayed abnormal activity and structural change, but the difference in brain activity between HZ and PHN is still not known.

Objectives: To identify regional brain activity changes in HZ and PHN brains with resting-state functional magnetic resonance imaging (rs-fMRI) technique, and to observe the differences between HZ and PHN patients.

Study Design: Observational study.

Setting: University hospital.

Methods: Regional homogeneity (ReHo) and fractional aptitude of low-frequency fluctuation (fALFF) methods were employed to analysis resting-state brain activity. Seventy-three age and gender matched patients (50 HZ, 23 PHN) and 55 healthy controls were enrolled. ReHo and fALFF changes were analyzed to detect the functional abnormality in HZ and PHN brains.

Results: Compared with healthy controls, HZ and PHN patients exhibited abnormal ReHo and fALFF values in classic pain-related brain regions (such as the frontal lobe, thalamus, insular, and cerebellum) as well as the brainstem, limbic lobe, and temporal lobe. When HZ developed to PHN, the activity in the vast area of the cerebellum significantly increased while that of some regions in the occipital lobe, temporal lobe, parietal lobe, and limbic lobe showed an apparent decrease.

Limitations: (a) Relatively short pain duration (mean 12.2 months) and small sample size ($n = 23$) for PHN group. (b) Comparisons at different time points (with paired t-tests) for each patient may minimize individual differences.

Conclusions: HZ and PHN induced local brain activity changed in the pain matrix, brainstem, and limbic system. HZ chronification induced functional change in the cerebellum, occipital lobe, temporal lobe, parietal lobe, and limbic lobe. These brain activity changes may be correlated with HZ-PHN transition.

Key words: Herpes zoster, postherpetic neuralgia, resting-state fMRI (rs-fMRI), regional homogeneity (ReHo), fractional aptitude of low-frequency fluctuation (fALFF)

Pain Physician 2017; 20:E687-E699

Herpes zoster (HZ) is characterized by a vesicular rash with a dermatomal distribution. Postherpetic neuralgia (PHN) is a neuropathic pain (NP) syndrome usually defined as chronic pain lasting more than 3 months following an outbreak of shingles (acute HZ) (1,2). This stabbing PHN pain profoundly affects the quality of life (3) and increases the economic burden on society (4). Moreover, PHN may increase the risk of anxiety, depression, and suicide (5,6). Understanding the brain activity in PHN patients will help to develop strategies for preventing and curing PHN.

The functional change between HZ and PHN in the brain is not clear. Some studies have explored PHN brain activity by using functional magnetic resonance imaging (fMRI) (7-9). Besides regions of the sensory-discriminative areas (10), brain areas (such as striatum, amygdala) associated with emotion, hedonics, and reward were also activated in PHN patients (7). Cerebral blood flow (CBF) was increased in the S1 area, inferior parietal lobule, insula, thalamus, amygdala, and striatum but decreased in the frontal cortex in PHN patients (11). Functional connectivity (FC) analysis indicated that connections between the putamen and some other regions were altered in PHN patients (8). Zhang et al (9) analyzed the small-world network (graphs with dense local connections and a few long connections) in the PHN brain with graph theoretic approaches. Decreased brain local efficiency and the regional nodal efficiency were found in brain areas related to sense, memory, and emotion (9). We previously found PHN patients exhibited significantly abnormal spontaneous brain activity in the pain matrix as well as the brainstem, limbic system, and temporal lobe (accepted by *Pain Physician*, in press). Because not all of the "abnormal" brain areas in PHN patients were pain specific, we hypothesized that in the process of transition from HZ to PHN, more pain nonspecific brain areas took part.

The regional homogeneity (ReHo) (12,13) and the fractional amplitude of the low frequency fluctuations (fALFF) (14,15) are powerful and reliable indices in evaluating resting-state brain activity (16-18), both of which can quantitatively measure local brain activity. ReHo, which was calculated by Kendall's coefficient of concordance (KCC), was first proposed by Zang et al (12) in 2004. ReHo evaluates similarities between time series of a given voxel and its nearest neighbors, therefore, ReHo reflects the local coherence of local spontaneous neuronal activity. On the other hand, the amplitude of the low frequency oscillation in the brain

reflects fundamental information of the resting-state brain activity. In addition, the power of low frequencies (e.g., the frequently used band 0.01 – 0.08 Hz) signals in the brain is proportional to the amplitudes of the blood oxygen level dependent (BOLD) signal. fALFF, which is measured by dividing the chosen low frequency band (e.g., 0.01 – 0.08 Hz) by all frequencies measured, have been developed as one index to characterize the low frequency oscillation amplitudes. fALFF has been proven to be more gray matter-specific and sensitive to BOLD signal (14).

In the present study, we employed ReHo and fALFF to detect local brain synchronicity and activity in HZ patients, PHN patients, and healthy controls, and compared the brain activity difference among the 3 groups.

METHODS

This resting-state fMRI (rs-fMRI) study was approved by the Ethics Committee of our local hospital.

Participants

All participants were right handed. Patients were recruited from the Pain Medicine Department of the local hospital from October 2014 to September 2016. The diagnosis of HZ and PHN was based on the International Association for the Study of Pain (IASP) criteria (19). Spontaneous pain intensity was assessed using the visual analog scale (VAS). All of the patients recruited in both groups suffered pain with VAS scores ≥ 5 , and no antidepressants or antipsychotic drugs were taken before MRI scans. All PHN patients reported persistent pain for more than 3 months after the HZ rash (shingles). All participants had no history of psychiatric or neurological disorder, and were free from any other kind of pain. Five patients were excluded for remarkable cerebral infarctions or head movement. All of the age and gender matched healthy controls were free from pain, and without brain structural abnormalities or neuropsychiatric disorders.

Image Acquisition

The fMRI experiments were implemented on a GE Signa HDxT 3.0 T MRI scanner (GE Company, USA) with a standard 8 channel head coil. fMRI data were acquired using an echo-planar image (EPI) sequence with parameters as follows: thickness/gap = 4.0/0 mm, matrix = 64 × 64, TR = 2000 ms, TE = 40 ms, flip angle = 90°, field of view (FOV) = 240 × 240 mm. A total of 210 time points and 33 axial slices were obtained in 7 minutes. High-resolution anatomic 3-D T1 (TR = 5.8 ms, TE

= 1.8 ms, flip angle = 12°, thickness/gap = 1.0/0 mm, 196 sagittal slices, FOV = 256 × 256 mm, matrix = 256 × 256) images were also acquired.

Image Processing

Preprocessing was performed using the Data Processing Assistant for Resting-State fMRI (DPARSF, <http://rest.restfmri.net/forum/DPARSF>) (20) and SPM8 (Wellcome Department, University College of London, UK) software based on MATLAB R2012a (MathWorks, USA). DPARSF was used for the following steps: To allow for the scanner calibration and participants' adaptation in the scan, the first 10 volumes were discarded and the remaining 200 volumes were further analyzed. Processing steps included slice timing, head-motion correction, spatial normalization to the Montreal Neurological Institute (MNI) space, and resampling with a 3 × 3 × 3 mm³ resolution. Participants with head motion > 2.0 mm of translation or > 2.0° of rotation in any direction were excluded from further processing. The linear trend of the fMRI data was removed. For ReHo analysis, the band-pass filtering (0.01 – 0.08 Hz) was conducted to discard high-frequency physiological noise and the frequency drift lower than 0.01 Hz (21). Resting State fMRI Data Analysis Toolkit (REST, <http://rest.restfmri.net>) (15) was used to conduct the subsequent steps: Individual ReHo map was generated by calculating the KCC of the time series of a given voxel with those of its neighbors (26 voxels) in a voxel-wise way (12,22). Afterwards, a whole-brain mask was adopted to remove the non-brain tissues. For standardization purposes, the individual ReHo maps were divided by their own global mean KCC within the whole-brain mask. Then spatial smoothing was performed on the standardized individual ReHo map with a Gaussian kernel of 4 mm full-width at half maximum (FWHM) (23). fALFF analysis was conducted as previously described (14,17). First, the resampled images were smoothed with a Gaussian kernel of 4 mm. Then the frequency band filtering was set as 0.01 – 0.08 Hz, and the time courses were converted to the frequency band using a Fast Fourier Transform.

The mean and standard deviation of each individual's ReHo and fALFF value was calculated by DPARSF within the whole brain mask. Z scores were then calculated in a voxel-wise way by subtracting the mean ReHo or fALFF values from each voxel's value, and then divided by the standard deviation of ReHo or fALFF value respectively. In this way, the Z score represents a voxel's ReHo or fALFF value in relation to all voxels in the whole brain. Therefore, the positive Z score represents higher synchronicity (ReHo) or activity (fALFF) in that individual's brain. Likewise, a negative Z score represents lower synchronicity or activity.

Statistical Analysis

Demographic and clinical data were analyzed using Prism 6.0 (GraphPad Software Inc, USA). Two-sample t-tests were used for detecting the differences in age. χ^2 test was applied for comparison of gender ratio. The criteria for all statistical significance were set as $P < 0.05$.

For ReHo and fALFF comparison, 2-sample t-tests were conducted in a whole-brain voxel-wise way with REST 1.8. To determine the significance of ReHo and fALFF between 2 groups, multiple comparison correction was performed by Monte Carlo simulations (24) using the REST AlphaSim utility (15). Voxels with $P < 0.05$ (2-tailed, corrected with AlphaSim method: rmm = 4 mm, cluster size > 1458 mm³ (54 voxels); <http://afni.nih.gov/afni/docpdf/AlphaSim.pdf>) were regarded as a significant difference.

REST Slice Viewer, which is routinely used for the display of statistic results (15), was used to generate graphs. Brain areas were overlaid on structural brain images. A color-bar was set to illustrate the statistic values (25).

RESULTS

Demographic and Clinical Features

Clinical characteristics of HZ and PHN patients are listed in Table 1. There were no remarkable differences in age ($P = 0.18, 0.15, 0.08$ for HZ vs Con, PHN vs Con,

Table 1. Demographic and clinical characteristics of participants.

	HZ patient N = 50	PHN patient N = 23	Healthy control N = 55
Age (year, mean ± SEM)	60.5 ± 1.8	65.9 ± 2.3	63.1 ± 0.79
Gender (male:female)	29:21	10:13	31:24
Pain duration (month, mean ± SEM)	0.98 ± 0.1	12.2 ± 3.7	-
VAS score (mean ± SEM)	6.8 ± 0.2	6.7 ± 0.3	-

HZ: herpes zoster; PHN: postherpetic neuralgia; VAS: visual analog scales; SEM: standard error of mean.

and PHN vs HZ respectively, 2-sample t-test) and gender ($P = 0.87, 0.30, 0.25$ for HZ vs Con, PHN vs Con, and PHN vs HZ respectively, χ^2 test) among the 3 groups.

Comparison of ReHo and fALFF between HZ and Control Group

As shown in Table 2 and Fig. 1, compared with controls, HZ brains showed significantly increased ReHo and fALFF values, mainly in the pons, frontal lobe (precentral gyrus and cingulate gyrus), thalamus, insula,

putamen, and midbrain. Lower ReHo and fALFF values were observed in the cerebellum, temporal lobe (Temporal_Inf), and frontal lobe (Frontal_Sup_Medial and Frontal_Inf_Orb).

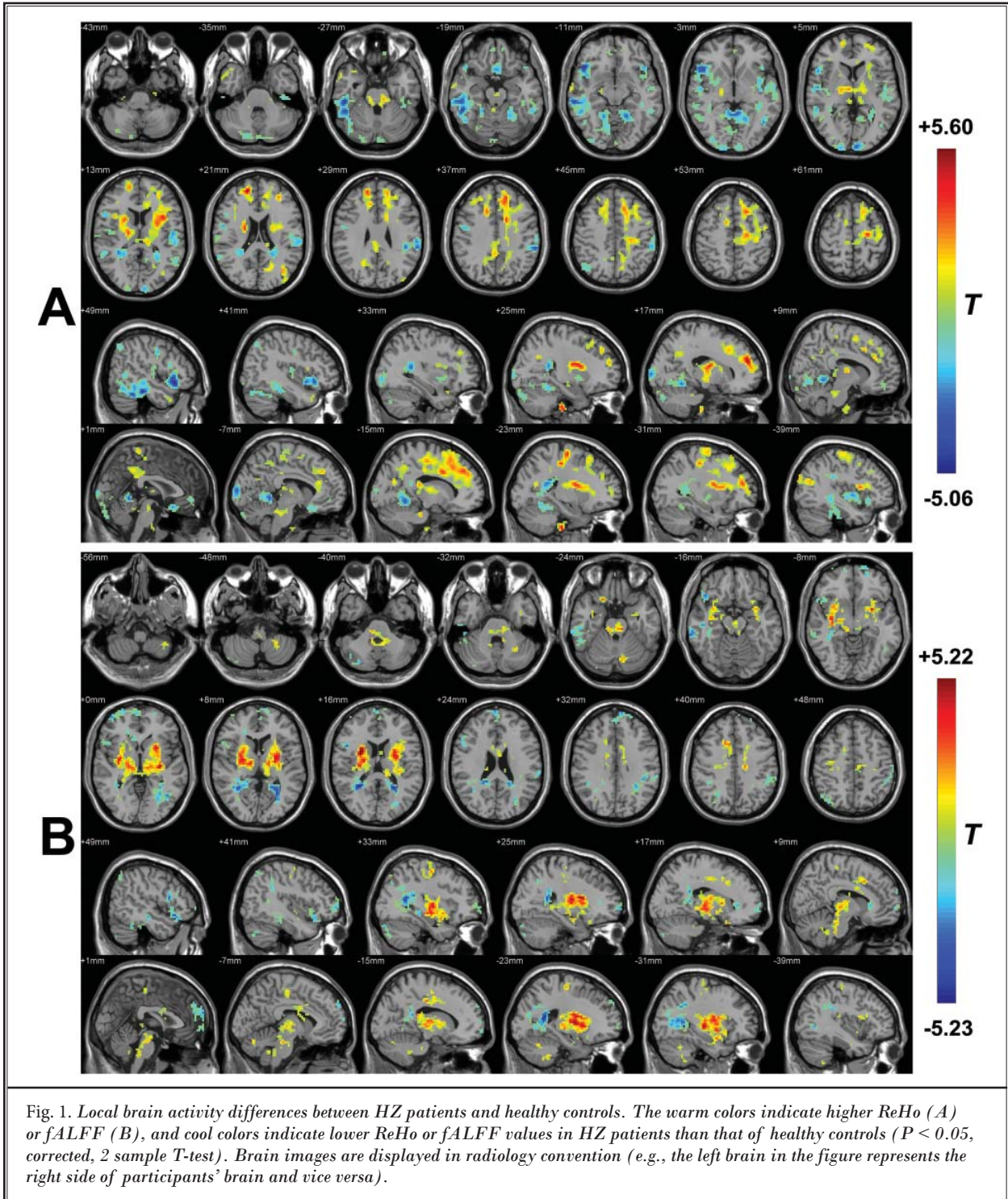
Comparison of ReHo and fALFF between PHN and Control Group

As shown in Table 3 and Fig. 2, PHN brains showed increased ReHo and fALFF values mainly in the vast area of the cerebellum, pons, frontal lobe (precentral gyrus

Table 2. Clusters of different ReHo or fALFF values between HZ and control group (Con).

Region (R: right; L: left)	Peak MNI coordinate			Peak T value	Voxel number	Brain volume (mm ³)
	x	y	z			
HZ > Con (ReHo)						
Temporal_Pole_Mid_R	57	9	-33	3.77	98	2646
Brainstem_L	-12	-27	-30	3.87	145	3915
Extra-Nuclear_R	21	-6	18	5.60	3088	83376
Frontal_Sup_R	18	51	21	5.28	608	16416
Occipital_Mid_L	-42	-87	27	3.83	102	2754
Limbic Lobe_R	3	-45	36	3.38	201	5427
HZ < Con (ReHo)						
Cerebelum_Crus2_R	21	-84	-33	-2.94	172	4644
Temporal_Inf_R	51	-30	-24	-5.06	2357	63639
SupraMarginal_L	-60	-36	33	-4.34	832	22464
Frontal_Med_Orb_L	0	45	-6	-2.80	66	1782
Frontal_Inf_Orb_R	48	21	-12	-4.86	431	11637
Occipital_Sup_R	18	-102	3	-3.63	166	4482
Occipital_Sup_L	-6	-99	6	-3.90	114	3078
Temporal_Mid_L	-45	-63	-3	-3.82	66	1782
Angular_R	39	-69	48	-2.95	65	1755
HZ > Con (fALFF)						
Putamen_R	30	-9	3	5.22	2381	64287
Cerebelum_Crus1_L	-9	-75	-24	3.32	57	1539
Cingulate Gyrus (bilateral)	-15	-18	39	3.72	219	5913
Precentral (bilateral)	36	-12	54	4.02	109	2943
HZ < Con (fALFF)						
Cerebellum Posterior Lob_R	36	-78	-45	-3.40	86	2322
Temporal_Inf_R	69	-33	-21	-4.60	247	6669
Temporal Lobe_R	27	-48	15	-5.23	468	12636
Frontal_Inf_Orb_R	48	21	-12	-4.37	178	4806
Frontal_Sup_Medial_R	3	66	21	-4.04	379	10233
Sub-Gyral (bilateral)	-24	-51	15	-5.10	537	14499
SupraMarginal_L	-63	-36	36	-3.40	107	2889
Angular_R	51	-63	42	-2.96	55	1485

ReHo: regional homogeneity; fALFF: fractional amplitude of low-frequency fluctuation; HZ: herpes zoster; MNI: Montreal Neurological Institute.



and midial frontal gyrus), thalamus, insula, putamen, precuneus, and midbrain compared to that of healthy controls. Lower ReHo and fALFF values were observed

in the limbic system (limbic lobe, cingulated gyrus), temporal lobe (Temporal_Inf), occipital lobe, and parietal lobe (Parietal_Inf, precuneus).

Table 3. Clusters of different ReHo or fALFF values between PHN and control group (Con).

Region (R: right; L: left)	Peak MNI coordinate			Peak T value	Voxel number	Brain volume (mm ³)
	x	y	z			
PHN > Con (ReHo)						
Pons_L	-12	-39	-33	5.15	879	23733
Cerebellum_L	-42	-78	-48	2.83	118	3186
Temporal_Pole_Mid_R	39	12	-33	3.49	64	1728
Frontal_Sup_Orb_R	21	27	-15	3.27	108	2916
Frontal_Sup_L	-12	30	39	6.09	4223	114021
Precuneus_R	3	-69	33	3.31	117	3159
Middle Temporal Gyrus_L	-42	-87	27	3.40	179	4833
PHN < Con (ReHo)						
Extra-Nuclear_L	-24	-48	18	-5.22	1420	38340
Cerebelum_Crus1_R	48	-39	-33	-6.73	4293	115911
Parietal_Inf_L	-57	-33	48	-5.54	826	22302
Supp_Motor_Area_L	0	-9	48	-3.41	69	1863
PHN > Con (fALFF)						
Cerebelum_8_L	-27	-57	-48	5.26	1524	41148
Temporal Lobe_R	30	-9	-42	4.81	244	6588
Temporal_Inf_L	-51	-9	-33	4.91	244	6588
Insula_L	-33	-18	3	5.55	672	18144
Extra-Nuclear_R	21	-15	3	6.39	553	14931
Middle Temporal Gyrus_L	-48	-75	21	3.86	126	3402
Precuneus_R	3	-72	39	4.35	56	1512
Cingulate Gyrus_L	-18	-9	42	4.81	632	17064
PHN < Con (fALFF)						
Precuneus_R	24	-48	12	-4.76	850	22950
Lingual_R	3	-81	-6	-3.58	216	5832
Occipital Lobe_L	-21	-60	6	-5.22	874	23598
Frontal_Inf_Orb_L	-45	18	-12	-4.12	55	1485
Frontal_Sup_Medial_R	3	57	15	-5.07	311	8397
Cingulate Gyrus_R	3	-18	27	-4.05	158	4266
Superior Frontal Gyrus_R	15	27	66	-4.83	129	3483

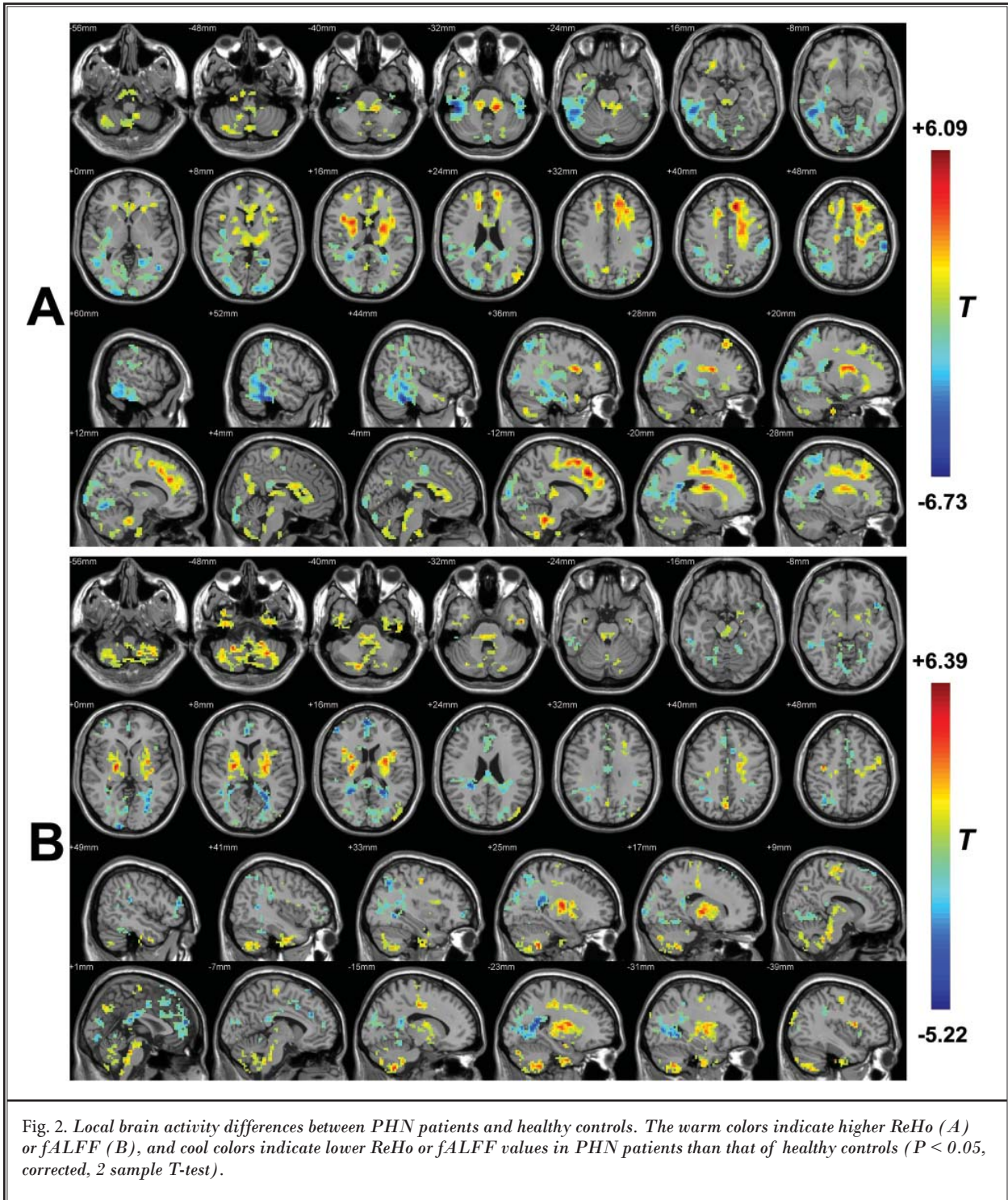
ReHo: regional homogeneity; fALFF: fractional amplitude of low-frequency fluctuation; PHN: postherpetic neuralgia; MNI: Montreal Neurological Institute.

Comparison of ReHo and fALFF between PHN and HZ Patients

As shown in Table 4 and Fig. 3, compared with HZ, PHN brain showed significantly increased ReHo and fALFF mainly in most of the cerebellum. Lower ReHo and fALFF values were observed in the limbic system (limbic lobe, cingulate gyrus), temporal lobe (Temporal_Mid), occipital lobe (middle occipital gyrus, Occipital_Mid), and parietal lobe (Parietal_Inf, Parietal_Sup).

DISCUSSION

As evidenced by ReHo and fALFF results, both HZ and PHN brains showed abnormal local connectivity and activity in several brain regions. Most of these brain areas, such as the frontal lobe, cerebellum, thalamus, insula, cingulate gyrus, and parietal lobe, belong to the "pain matrix," which was defined as regions that exhibited a reliable activation in response to increasing levels of pain (10,26-28). The pain matrix includes the somatosensory area, supplementary motor area,



cerebellum, forebrain, thalamus, insula, anterior cingulate gyrus (ACC), posterior parietal cortex, periaqueductal grey, and striatum (29,30). Tables 2 – 3 and Figs.

1 – 2 show that besides the regions belonging to the pain matrix, the brainstem and some other regions of the limbic system (limbic lobe, hippocampus, parahip-

Table 4. Clusters of different ReHo or fALFF values between PHN and HZ patients.

Region (R: right; L: left)	Peak MNI coordinate			Peak T value	Voxel number	Brain volume (mm ³)
	x	y	z			
PHN > HZ (ReHo)						
Cerebelum_9_L	-9	-51	-54	4.42	255	6885
Cerebelum_7b_R	36	-66	-48	4.19	375	10125
Cerebelum_Crus2_L	-39	-81	-42	3.47	86	2322
Fusiform_L	-24	-42	-18	3.95	86	2322
Rectus_L	-9	51	-18	3.92	70	1890
PHN < HZ (ReHo)						
Temporal_Mid_R	51	-45	-6	-4.23	201	5427
Middle Occipital Gyrus_R	36	-78	6	-3.35	212	5724
Occipital_Mid_L	-36	-81	3	-3.51	181	4887
Posterior Cingulate_L	-3	-36	24	-2.76	86	2322
Angular_R	30	-60	51	-4.67	608	16416
Parietal_Sup_L	-33	-48	63	-3.85	395	10665
Cerebelum_Crus1_R	45	-39	-33	-4.32	264	7128
PHN > HZ (fALFF)						
Cerebelum_Crus2_L	-39	-72	-48	4.56	1246	33642
Precentral_R	15	-27	75	3.16	56	1512
PHN < HZ (fALFF)						
Cingulum_Mid_L	-9	9	33	-3.84	312	8424
Parietal_Inf_R	51	-33	54	-3.53	97	2619
Parietal_Sup_R	21	-63	51	-3.53	122	3294

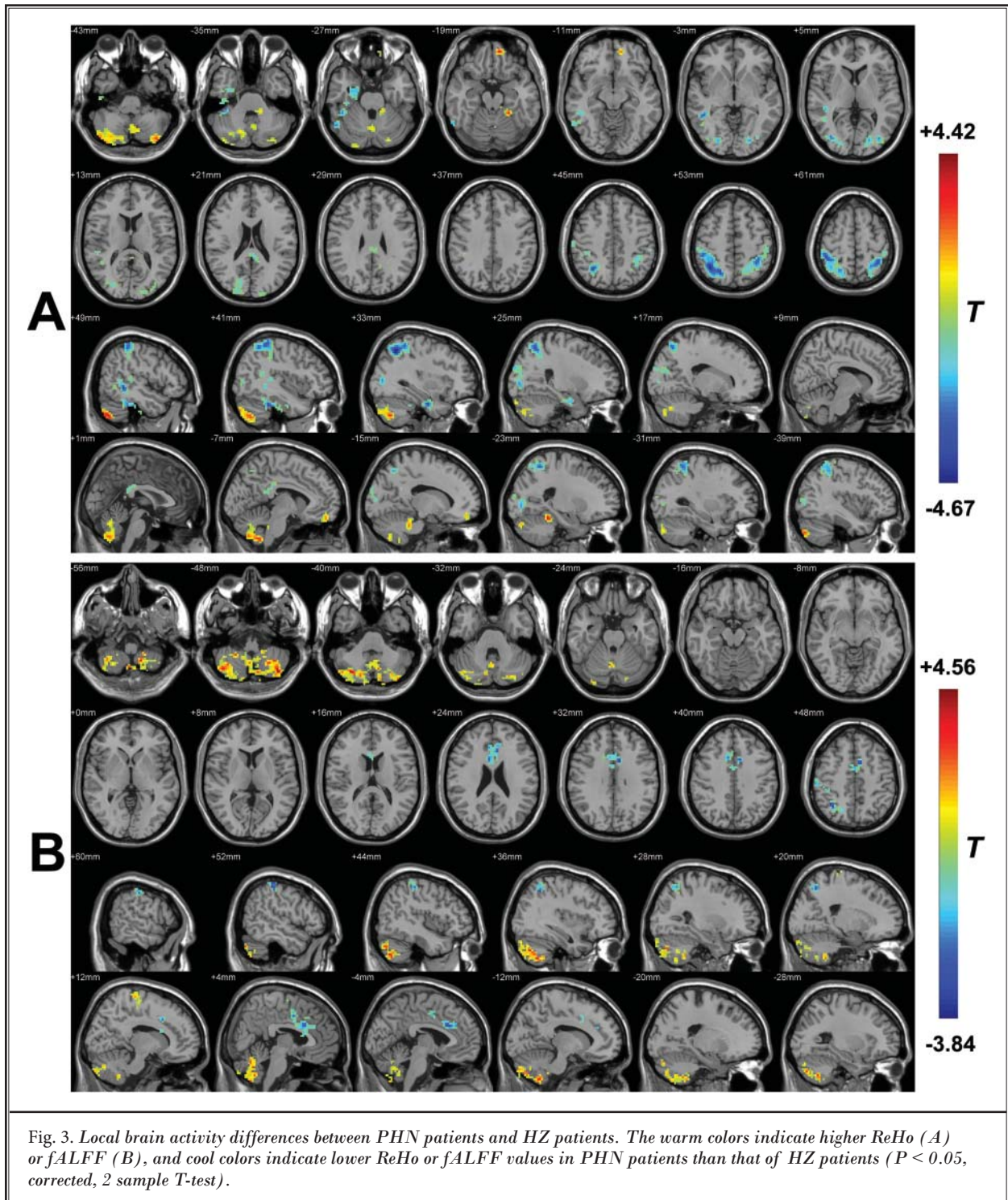
ReHo: regional homogeneity; fALFF: fractional amplitude of low-frequency fluctuation; PHN: postherpetic neuralgia; HZ: herpes zoster; MNI: Montreal Neurological Institute.

pocampal gyrus, amygdale, et al) were also involved. This suggests that HZ and PHN not only influence brain areas of pain perception, but also more complex brain mechanisms exist in HZ and PHN pathogenesis.

As we expected, HZ and PHN brains displayed different functional styles. Interestingly, HZ chronification (PHN state) resulted in a significant cerebellum activity increase. In addition, PHN brains showed a low brain activity in the limbic system, temporal lobe, occipital lobe, and parietal lobe. It suggests that these brain areas may participate in the transition from PHN to HZ.

The limbic regions of the pain matrix encode emotional aspects of pain perception, and the primary sensory region encodes the intensity of pain sensation (31,32). Chronic pain studies in rodents showed functional changes in limbic regions (the hippocampus [33-36], amygdala [37], striatum [38], and frontal cortex [39-41]). Whole-brain network analysis of NP rats showed FC changes within the limbic system and between the limbic and nociceptive systems (42). Recent human imaging results (7,9,43,44) displayed the same trend.

Indicated with ReHo and fALFF values, the brainstem was activated both in HZ and PHN states. The brainstem is one major site of pain processing and modulation. It contains many nuclei, which project to the spinal dorsal horn and vast area of the brain. For example, the noradrenergic locus coeruleus (LC), which is located at the pons, is a relevant structure in modulating both ascending and descending pain. By sending to dorsal horn, LC forms one of the noradrenergic pontospinal descending pain inhibition pathways, which reduces the spinal transmission of noxious inputs (45-47). The LC is the primary source of norepinephrine (NE) in the brain. LC produces NE and releases it to vast regions of the brain to maintain the cortical activation and behavioral arousal (48). LC, the central "stress circuitry," influences depression and anxiety disorders (49). The activity of the LC-prefrontal cortex (PFC) noradrenergic neurons increased in the NP state (50). Plastic changes in the descending noradrenergic inhibitory system have been reported in NP rats (51,52).



The cerebellum is part of the pain matrix and it is always activated in painful events in healthy humans (53) and in patients with chronic pain (54). For example,

neuralgia (mononeuropathy) could induce an increased rCBF in the cerebellum (55). Kim et al (56) found that cerebellar activity correlated well with rat NP develop-

ment in an 8-week longitudinal FDG microPET imaging study. More interestingly, the cerebellum is linked to depression (57). Abnormal cerebellar response to the anticipation of pain has been suggested to be a potential marker for depression (58). Patients with depression showed increased resting activity in the cerebellum (59). These studies suggest that pain and depression may share a common mechanism within the cerebellum (57), in addition, the cerebellum holds the potential to be one target for chronic pain treatment. For example, Bocci et al (60) have reported that cerebellar direct current stimulation (tDCS) could modulate pain perception and its cortical correlates.

Many of the ReHo and fALFF activity abnormal regions in this work hold additional functions besides pain processing. For example, the prefrontal lobe is associated with depression and anxiety (61). The limbic system and brainstem are involved in sleep control (62). Pain is an integrated feeling of sensory, affective, and cognitive dimensions (63). As one kind of NP, PHN is not just about somatic and affective pain characteristics. Geha et al (7) analyzed the BOLD signal of PHN patients and detected that brain areas with BOLD change were not restricted to the sensory-discriminative areas, but also the emotion, reward, and punishment related brain regions. It is well known that chronic pain and neuropsychiatric diseases such as depression (64) and anxiety (65), cognitive dysfunctions (66), and sleep disorder (67) are highly comorbid. Indeed, up to 50% of patients with chronic pain exhibited symptoms of anxiety or depression (68), whereas in some studies the number reached to 75% (69). Importantly, the prevalence of depression increased with greater pain severity (64). Sleep disorder is another complication in chronic pain patients. Patients may experience sleep problems after they suffer chronic pain. It is reported that more than half of chronic neck pain patients experienced mild to severe insomnia (70). Conversely, inadequate sleep due to NP may contribute to living with chronic pain (71,72). Considering the above mentioned functional neuronal

change in HZ and PHN patients, we predict that HZ and PHN patients not only experience physical and affective pain, but are likely to suffer mood disorders.

Although much of the brain image studies of PHN were conducted using fMRI, we should notice that ample evidence indicated that NP resulted in (at least accompanied by) plastic change in human (73-77) and murine (78,79) brains. Most of the plastic or structural alterations took place in pain-processing regions. For instance, when NP leads to anxio-depressive-like behaviors, it impaired the noradrenergic pathway as evidenced by the plastic change in LC (80). We found that PHN patients showed abnormal microstructure in the occipital lobe, middle frontal gyrus, superior temporal gyrus, parahippocampal gyrus, insula, thalamus, cerebellum anterior lobe, and caudate as evidenced by decreased diffusional kurtosis imaging (DKI) intensity (25). It will be useful analyze the underlying molecular mechanisms in the aforementioned brain regions.

Limitations

For the PHN group, the sample size (23 patients) is limited and pain duration (mean 12.2 months) is still short. Although it is not easy to enroll patients who suffer from acute HZ to chronic PHN pain, we think it is an effective way to eliminate confounding factors such as individual differences, which will affect the reliability of fMRI results. It is important to notice that fMRI study with conventional software may hold a high false-positive rate (81), alternative neuroscience technologies are warranted to identify the function of above mentioned brain areas in HZ and PHN conditions.

CONCLUSIONS

HZ and PHN patients displayed abnormal brain activity in brain regions related to sensory as well as emotional processes. Functional change in the cerebellum, occipital lobe, temporal lobe, parietal lobe, and limbic lobe is one feature of the HZ-PHN transition, which indicates PHN is not all about pain in brain.

REFERENCES

1. Keating GM. Shingles (herpes zoster) vaccine (Zostavax®): A review in the prevention of herpes zoster and postherpetic neuralgia. *BioDrugs* 2016; 30:1-12.
2. Cohen JL. Herpes zoster. *N Engl J Med* 2013; 369:255-263.
3. Pickering G, Gavazzi G, Gaillat J, Paccalin M, Bloch K, Bouhassira D. Is herpes zoster an additional complication in old age alongside comorbidity and multiple medications? Results of the post hoc analysis of the 12-month longitudinal prospective observational ARIZONA cohort study. *BMJ Open* 2016; 6:e009689.
4. Friesen KJ, Falk J, Alessi-Severini S, Chateau D, Bugden S. Price of pain: Population-based cohort burden of disease analysis of medication cost of herpes zoster and postherpetic neuralgia. *J Pain Res* 2016; 9:543.
5. Sah DWY, Ossipo MH, Frank P. Neurotrophic factors as novel therapeutics for neuropathic pain. *Nat Rev Drug Discov* 2003; 2:460-472.

6. Denkinger MD, Lukas A, Nikolaus T, Peter R, Franke S, Group AS. Multisite pain, pain frequency and pain severity are associated with depression in older adults: Results from the ActiFE Ulm study. *Age Ageing* 2014; 43:510-514.
7. Geha PY, Baliki MN, Chialvo DR, Harden RN, Paice JA, Apkarian AV. Brain activity for spontaneous pain of postherpetic neuralgia and its modulation by lidocaine patch therapy. *Pain* 2007; 128:88-100.
8. Geha PY, Baliki MN, Wang X, Harden RN, Paice JA, Apkarian AV. Brain dynamics for perception of tactile allodynia (touch-induced pain) in postherpetic neuralgia. *Pain* 2008; 138:641-656.
9. Zhang Y, Liu J, Li L, Du M, Fang W, Wang D, Jiang X, Hu X, Zhang J, Wang X. A study on small-world brain functional networks altered by postherpetic neuralgia. *Magn Reson Imaging* 2014; 32:359-365.
10. Peyron R, Laurent B, García-Larrea L. Functional imaging of brain responses to pain. A review and meta-analysis. *Neurophysiol Clin* 2000; 30:263-288.
11. Liu J, Hao Y, Du M, Wang X, Zhang J, Manor B, Jiang X, Fang W, Wang D. Quantitative cerebral blood flow mapping and functional connectivity of postherpetic neuralgia pain: A perfusion fMRI study. *Pain* 2013; 154:110-118.
12. Zang Y, Jiang T, Lu Y, He Y, Tian L. Regional homogeneity approach to fMRI data analysis. *Neuroimage* 2004; 22:394-400.
13. Zuo XN, Xu T, Jiang L, Yang Z, Cao XY, He Y, Zang YF, Castellanos FX, Milham MP. Toward reliable characterization of functional homogeneity in the human brain: Preprocessing, scan duration, imaging resolution and computational space. *Neuroimage* 2013; 65:374-386.
14. Zou QH, Zhu CZ, Yang Y, Zuo XN, Long XY, Cao QJ, Wang YF, Zang YF. An improved approach to detection of amplitude of low-frequency fluctuation (ALFF) for resting-state fMRI: Fractional ALFF. *J Neurosci Methods* 2008; 172:137-141.
15. Song XW, Dong ZY, Long XY, Li SF, Zuo XN, Zhu CZ, He Y, Yan CG, Zang YF. REST: A toolkit for resting-state functional magnetic resonance imaging data processing. *Plos One* 2011; 6:e25031.
16. Fryer SL, Roach BJ, Ford JM, Turner JA, Erp TGMV, Voyvodic J, Preda A, Belger A, Bustillo J, O'Leary D. Relating intrinsic low-frequency BOLD cortical oscillations to cognition in schizophrenia. *Neuropsychopharmacology* 2015; 40:2705-2714.
17. Haag LM, Heba S, Lenz M, Glaubitz B, Höffken O, Kalisch T, Puts NA, Edden RAE, Tegenthoff M, Dinse H. Resting BOLD fluctuations in the primary somatosensory cortex correlate with tactile acuity. *Cortex* 2015; 64:20-28.
18. Ying C, Yun J, Yu-Chen C, Kun W, Bo G, Song W, Shenghong J, Gao-Jun T. Altered spontaneous brain activity in type 2 diabetes: A resting-state functional MRI study. *Diabetes* 2014; 63:749-760.
19. Merskey H, Bogduk N. *Classification of Chronic Pain: Descriptions of Chronic Pain Syndromes and Definitions of Pain Terms*. Ed 2. International Association for the Study of Pain, Seattle, 1994.
20. Yan C, Zang Y. DPARSF: A MATLAB toolbox for "pipeline" data analysis of resting-state fMRI. *Front Syst Neurosci* 2010; 4:13.
21. Greicius MD, Ben K, Reiss AL, Vinod M. Functional connectivity in the resting brain: A network analysis of the default mode hypothesis. *Proc Natl Acad Sci U S A* 2003; 100:253-258.
22. Li Z, Kadivar A, Pluta J, Dunlop J, Wang Z. Test-retest stability analysis of resting brain activity revealed by blood oxygen level-dependent functional MRI. *J Magn Reson Imaging* 2012; 36:344-354.
23. Wang L, Li K, Zhang Q, Zeng Y, Dai W, Su Y, Wang G, Tan Y, Jin Z, Yu X. Short-term effects of escitalopram on regional brain function in first-episode drug-naïve patients with major depressive disorder assessed by resting-state functional magnetic resonance imaging. *Psychol Med* 2014; 44:1417-1426.
24. Ledberg A, Åkerman S, Roland PE. Estimation of the probabilities of 3D clusters in functional brain images. *Neuroimage* 1998; 8:113-128.
25. Zhang Y, Yu T, Qin B, Li Y, Song G, Yu B. Microstructural abnormalities in gray matter of patients with postherpetic neuralgia: A diffusional kurtosis imaging study. *Pain Physician* 2016; 19:E601-E611.
26. Jensen KB, Kosek E, Wicksell R, Kemani M, Olsson G, Merle JV, Kadetoff D, Ingvar M. Cognitive behavioral therapy increases pain-evoked activation of the prefrontal cortex in patients with fibromyalgia. *Pain* 2012; 153:1495-1503.
27. Treede RD, Kenshalo DR, Gracely RH, Jones AK. The cortical representation of pain. *Pain* 1999; 79:105-111.
28. Seifert F, Maihöfner C. Central mechanisms of experimental and chronic neuropathic pain: Findings from functional imaging studies. *Cell Mol Life Sci* 2009; 66:375-390.
29. Garcia-Larrea L, Peyron R. Pain matrices and neuropathic pain matrices: A review. *Pain* 2013; 154:S29-S43.
30. Legrain V, Iannetti GD, Plaghki L, Mouraux A. The pain matrix reloaded: A salience detection system for the body. *Prog Neurobiol* 2011; 93:111-124.
31. Price DD. Psychological and neural mechanisms of the affective dimension of pain. *Science* 2000; 288:1769-1772.
32. Rainville P, Duncan GH, Price DD, Carrier B, Bushnell MC. Pain affect encoded in human anterior cingulate but not somatosensory cortex. *Science* 1997; 277:968-971.
33. Adriana DR, Hau-Jie Y, Anke R, Centeno MV, Johannes W, Marco M, Besedovsky HO, A Vania A. Chronic neuropathic pain-like behavior correlates with IL-1 β expression and disrupts cytokine interactions in the hippocampus. *Pain* 2011; 152:2827-2835.
34. Mutso AA, Daniel R, Baliki MN, Lejman H, Ghazal B, Centeno MV, Jelena R, Marco M, Miller RJ, A Vania A. Abnormalities in hippocampal functioning with persistent pain. *J Neurosci* 2012; 32:5747-5756.
35. Carmen RG, Esther B, Cristina AD, Madrigal JLM, Perez-Nievas BG, Juan Carlos L, Juan Antonio M. Stress increases the negative effects of chronic pain on hippocampal neurogenesis. *Anesth Analg* 2015; 121:1078-1088.
36. Ren W-J, Liu Y, Zhou L-J, Li W, Zhong Y, Pang R-P, Xin W-J, Wei X-H, Wang J, Zhu H-Q. Peripheral nerve injury leads to working memory deficits and dysfunction of the hippocampus by upregulation of TNF- α in rodents. *Neuropsychopharmacology* 2011; 36:979-992.
37. Ren W, Palazzo E, Maione S, Neugebauer V. Differential effects of mGluR7 and mGluR8 activation on pain-related synaptic activity in the amygdala. *J Ind Microbiol Biot* 2011; 61:1334-1344.
38. Goffer Y, Xu D, Eberle SE, D'amour J, Lee M, Tukey D, Froemke RC, Ziff EB, Wang J. Calcium-permeable AMPA receptors in the nucleus accumbens regulate depression-like behaviors in the chronic neuropathic pain state. *J Neurosci* 2013; 33:19034-19044.
39. Pais-Vieira M, Aguiar P, Lima D, Galhardo V. Inflammatory pain disrupts the orbitofrontal neuronal activity and risk-as-

- essment performance in a rodent decision-making task. *Pain* 2012; 153:1625-1635.
40. Metz AE, Hau-Jie Y, Maria Virginia C, A Vania A, Marco M. Morphological and functional reorganization of rat medial prefrontal cortex in neuropathic pain. *Proc Natl Acad Sci U S A* 2009; 106:2423-2428.
 41. Seminowicz DA, Laferriere AM. MRI structural brain changes associated with sensory and emotional function in a rat model of long-term neuropathic pain. *Neuroimage* 2009; 47:1007-1014.
 42. Baliki MN, Chang PC, Baria AT, Centeno MV, Apkarian AV. Resting-state functional reorganization of the rat limbic system following neuropathic injury. *Sci Rep* 2014; 4:6186.
 43. Baliki MN, Bogdan P, Souraya T, Herrmann KM, Lejian H, Schnitzer TJ, Fields HL, A Vania A. Corticostriatal functional connectivity predicts transition to chronic back pain. *Nat Neurosci* 2012; 15:1117-1119.
 44. Mansour AR, Baliki MN, Lejian H, Souraya T, Herrmann KM, Schnitzer TJ, A Vania A. Brain white matter structural properties predict transition to chronic pain. *Pain* 2013; 154:2160-2168.
 45. Millan MJ. Descending control of pain. *Prog Neurobiol* 2002; 66:355-474.
 46. Hickey L, Li Y, Fyson SJ, Watson TC, Perrins R, Hewinson J, Teschemacher AG, Furue H, Lumb BM, Pickering AE. Optoactivation of locus ceruleus neurons evokes bidirectional changes in thermal nociception in rats. *J Neurosci* 2014; 34:4148-4160.
 47. Khan HS, Stroman PW. Inter-individual differences in pain processing investigated by functional magnetic resonance imaging of the brainstem and spinal cord. *Neuroscience* 2015; 307:231-241.
 48. Franks NP. General anaesthesia: From molecular targets to neuronal pathways of sleep and arousal. *Nat Revs Neurosci* 2008; 9:370-386.
 49. Shibata E, Sasaki M, Tohyama K, Otsuka K, Jin E, Terayama Y, Sakai A. Use of neuromelanin-sensitive MRI to distinguish schizophrenic and depressive patients and healthy individuals based on signal alterations in the substantia nigra and locus ceruleus. *Biol Psychiatry* 2008; 64:401-406.
 50. Koh K, Hamada A, Hamada Y, Yanase M, Sakaki M, Someya K, Narita M, Kuzumaki N, Ikegami D, Sakai H. Possible involvement of activated locus coeruleus-noradrenergic neurons in pain-related sleep disorders. *Neurosci Lett* 2015; 589:200-206.
 51. Hayashida K-i, Clayton BA, Johnson JE, Eisenach JC. Brain derived nerve growth factor induces spinal noradrenergic fiber sprouting and enhances clonidine analgesia following nerve injury in rats. *Pain* 2008; 136:348-355.
 52. Hughes S, Hickey L, Hulse R, Lumb B, Pickering A. Endogenous analgesic action of the pontospinal noradrenergic system spatially restricts and temporally delays the progression of neuropathic pain following tibial nerve injury. *Pain* 2013; 154:1680-1690.
 53. Helmchen C, Mohr C, Erdmann C, Petersen D, Nitschke M. Differential cerebellar activation related to perceived pain intensity during noxious thermal stimulation in humans: A functional magnetic resonance imaging study. *Neurosci Lett* 2003; 335:202-206.
 54. Jensen KB, Regenbogen C, Ohse MC, Frasnelli J, Freiherr J, Lundström JN. Brain activations during pain: A neuroimaging meta-analysis of patients with pain and healthy controls. *Pain* 2016; 157:1279-1286.
 55. Hsieh J-C, Belfrage M, Stone-Elander S, Hansson P, Ingvar M. Central representation of chronic ongoing neuropathic pain studied by positron emission tomography. *Pain* 1995; 63:225-236.
 56. Kim J, Shin J, Oh J-H, Jung HH, Kim Y-B, Cho Z-H, Chang JW. Longitudinal FDG microPET imaging of neuropathic pain: Does cerebellar activity correlate with neuropathic pain development in a rat model? *Acta Neurochir (Wien)* 2015; 157:1051-1057.
 57. Moulton EA, Schmahmann JD, Becerra L, Borsook D. The cerebellum and pain: Passive integrator or active participant? *Brain Res Rev* 2010; 65:14-27.
 58. Smith KA, Ploghaus A, Cowen PJ, McCleery JM, Goodwin GM, Smith S, Tracey I, Matthews PM. Cerebellar responses during anticipation of noxious stimuli in subjects recovered from depression. *Br J Psychiatry* 2002; 181:411-415.
 59. Fitzgerald PB, Laird AR, Maller J, Daskalakis ZJ. A meta-analytic study of changes in brain activation in depression. *Hum Brain Mapp* 2008; 29:683-695.
 60. Bocci T, Santarcangelo E, Vannini B, Torzini A, Carli G, Ferrucci R, Priori A, Valeriani M, Sartucci F. Cerebellar direct current stimulation modulates pain perception in humans. *Restor Neurol Neurosci* 2015; 33:597-609.
 61. Vincent V, Bagot RC, Cahill ME, Devereux F, Robison AJ, Dietz DM, Barbara F, Michelle MR, Ku SM, Eileen H. Prefrontal cortical circuit for depression- and anxiety-related behaviors mediated by cholecystokinin: Role of Δ FosB. *J Neurosci* 2014; 34:3878-3887.
 62. Zhang Z, Ferretti V, Güntan İ, Moro A, Steinberg EA, Ye Z, Zecharia AY, Yu X, Vyssotski AL, Brickley SG. Neuronal ensembles sufficient for recovery sleep and the sedative actions of [alpha]2 adrenergic agonists. *Nat Neurosci* 2015; 18:553-561.
 63. Melzack R. From the gate to the neuro-matrix. *Pain* 1999; suppl 6:S121-S126.
 64. Currie SR, Jianli W. More data on major depression as an antecedent risk factor for first onset of chronic back pain. *Psychol Med* 2005; 35:1275-1282.
 65. McWilliams LA, Cox BJ, Enns MW. Mood and anxiety disorders associated with chronic pain: An examination in a nationally representative sample. *Pain* 2003; 106:127-133.
 66. Coppieters I, Ickmans K, Cagnie B, Nijs J, De PR, Noten S, Meeus M. Cognitive performance is related to central sensitization and health-related quality of life in patients with chronic whiplash-associated disorders and fibromyalgia. *Pain Physician* 2015; 18:E389-E401.
 67. Morin CM, Gibson D, Wade J. Self-reported sleep and mood disturbance in chronic pain patients. *Clin J Pain* 1998; 14:311-314.
 68. Banks SM, Kerns RD. Explaining high rates of depression in chronic pain: A diathesis-stress framework. *Psychol Bull* 1996; 119:95-110.
 69. Sigtermans MJ, Hilten JJ, Van, Bauer MCR, M Sesmu A, Johan M, Sarton EY, Albert D. Ketamine produces effective and long-term pain relief in patients with complex regional pain syndrome type 1. *Pain* 2009; 145:304-311.
 70. Kim SH, Lee DH, Yoon KB, An JR, Yoon DM. Factors associated with increased risk for clinical insomnia in patients with chronic neck pain. *Pain Physician* 2015; 18:593-598.
 71. Odo M, Koh K, Takada T, Yamashita A, Narita M, Kuzumaki N, Ikegami D, Sakai H, Iseki M, Inada E. Changes in circadian rhythm for mRNA expression of melatonin 1A and 1B receptors in the hypothalamus under a neuropathic pain-like state. *Synapse* 2014; 68:153-158.
 72. Yamashita A, Hamada A, Suhara Y, Kaw-

- abe R, Yanase M, Kuzumaki N, Narita M, Matsui R, Okano H, Narita M. Astrocytic activation in the anterior cingulate cortex is critical for sleep disorder under neuropathic pain. *Synapse* 2014; 68:235-247.
73. Doan L, Manders T, Wang J. Neuroplasticity underlying the comorbidity of pain and depression. *Neural Plasticity* 2015; 2015:504691.
74. Goswami R, Anastakis DJ, Katz J, Davis KD. A longitudinal study of pain, personality and brain plasticity following peripheral nerve injury. *Pain* 2015; 157:729-739.
75. Desouza DD, Davis KD, Hodaie M. Reversal of insular and microstructural nerve abnormalities following effective surgical treatment for trigeminal neuralgia. *Pain* 2015; 156:1112-1123.
76. Sinding C, Gransjøen AM, Schlumberger G, Grushka M, Frasnelli J, Singh PB. Grey matter changes of the pain matrix in patients with burning mouth syndrome. *Eur J Neurosci* 2016; 43:997-1005.
77. Khan SA, Keaser ML, Meiller TF, Seminowicz DA. Altered structure and function in the hippocampus and medial prefrontal cortex in patients with burning mouth syndrome. *Pain* 2014; 155:1472-1480.
78. Dellarole A, Morton P, Brambilla R, Walters W, Summers S, Bernardes D, Grilli M, Bethea JR. Neuropathic pain-induced depressive-like behavior and hippocampal neurogenesis and plasticity are dependent on TNFR1 signaling. *Brain Behav Immun* 2014; 41:65-81.
79. Qiu S, Chen T, Koga K, Guo Y-y, Xu H, Song Q, Wang J-j, Descalzi G, Kaang B-K, Luo J-h. An increase in synaptic NMDA receptors in the insular cortex contributes to neuropathic pain. *Sci Signal* 2013; 6:ra34-ra34.
80. Alba-Delgado C, Llorca-Torralba M, Horrillo I, Ortega JE, Mico JA, Sánchez-Blázquez P, Meana JJ, Berrocoso E. Chronic pain leads to concomitant noradrenergic impairment and mood disorders. *Biol Psychiatry* 2013; 73:54-62.
81. Eklund A, Nichols TE, Knutsson H. Cluster failure: Why fMRI inferences for spatial extent have inflated false-positive rates. *Proc Natl Acad Sci U S A* 2016; 113:7900-7905.